



Parallel-quadrature phase-shifting digital holographic microscopy using polarization beam splitter

Bhargab Das, Chandra S. Yelleswarapu, D.V.G.L.N. Rao *

Physics Department, University of Massachusetts Boston, MA 02125, USA

ARTICLE INFO

Article history:

Received 11 May 2012

Received in revised form

23 July 2012

Accepted 25 July 2012

Available online 21 August 2012

Keywords:

Digital holography

Microscopy

Phase shifting

Image reconstruction techniques

ABSTRACT

We present a digital holography microscopy technique based on a parallel-quadrature phase-shifting method. Two $\pi/2$ phase-shifted holograms are recorded simultaneously using polarization phase-shifting principle, slightly off-axis recording geometry, and two identical CCD sensors. The parallel phase-shifting is realized by combining circularly polarized object beam with a 45° degree polarized reference beam through a polarizing beam splitter. DC term is eliminated by subtracting the two holograms from each other and the object information is reconstructed after selecting the frequency spectrum of the real image. Both amplitude and phase object reconstruction results are presented. Simultaneous recording eliminates phase errors caused by mechanical vibrations and air turbulences. The slightly off-axis recording geometry with phase-shifting allows a much larger dimension of the spatial filter for reconstruction of the object information. This leads to better reconstruction capability than traditional off-axis holography.

© 2012 Elsevier B.V. All rights reserved.

1. Introduction

Digital holographic microscopy (DHM) has emerged as a non-destructive, full-field, and label-free imaging technique for achieving quantitative phase imaging with high axial resolution and diffraction limited transverse resolution [1–9]. In DHM, interference pattern between the object and reference beam is digitally recorded using a CCD/CMOS sensor and the whole object information (quantitative phase and amplitude) is extracted by performing a numerical reconstruction using a computer [10]. However, the recorded digital hologram contains unwanted dc and twin-image diffracted waves. Several methods have been developed to eliminate these undesired diffracted waves and reconstruct the desired sample field (i.e. object wavefront). In the off-axis DHM, it is achieved by having a large angle between the object and reference waves [3,10,11]. Major advantage with this technique is that a single interferogram is sufficient for numerical reconstruction of the object information making it suitable for live cell dynamic studies. However, due to the large angle between object and reference beams this technique does not completely utilize the available space-bandwidth product (SBP) of the detector. Thus the higher spatial frequency components of the object might be lost [12–14] and hence from an

imaging point of view the resolution of the reconstructed image will be lower. The elimination of zero-order intensity and the twin image in off-axis holograms can also be performed by spatial phase-shifting based methods [15]. However such techniques require information concerning the spatial distribution of the phase difference between the object wave and the reference wave in the hologram plane.

This problem can be circumvented by using an in-line geometry in which the angle between the object and reference beam is set to zero. But this “in-line” geometry makes the undesired diffracted waves occlude the desired object field. Hence three or four phase-shifted holograms of the same object are recorded by introducing stepwise phase retardations in the reference beam [3,16]. Although this procedure enables to remove the dc and the twin image diffracted waves, but due to the sequential nature of recording the holograms, it is not suitable for simultaneous measurement of moving objects or dynamic process. In addition, it has been shown that calibration errors in phase-shifting and system fluctuations between the frames degrade the quality of the reconstructed image [17–20]. To overcome this difficulty, different types of parallel phase-shifting methods are proposed which can record the phase-shifted interferograms without any time lag. In one of the methods, four CCD detectors are employed for simultaneous recording of four phase-shifted interferograms [21–25]. Methods based on single CCD detector have also been demonstrated for simultaneous recording of the required number of interferograms by utilizing special optical components such as micro-polarizer array [26–28] and two-dimensional diffraction

* Corresponding author. Tel.: +1 617 287 6065; fax: +1 617 287 6053.

E-mail addresses: Bhargab.das@gmail.com (B. Das), Chandra.yelleswarapu@umb.edu (C.S. Yelleswarapu), raod@umb.edu (D.V.G.L.N. Rao).

grating [29,30]. The use of four CCD sensors to perform four-step phase shifting leads to complex system configuration and the technique of recording four phase-shifted holograms by a single CCD leads to under-utilization of the field of view of the CCD sensor. Techniques based on micro-polarizer array and phase gratings depend on the effectiveness of these array devices in generating multiple copies of the object and reference beams.

Shaked et al. proposed a two-step phase-shifting interferometry with slightly off-axis configuration where the dc term is successfully suppressed by subtracting one phase-shifted hologram from the other [31,32]. The reconstruction of the object information is based on the Hilbert transformation and hence requires a sinusoidal fringe pattern over the interferogram area. Thus this method is valid only for transparent objects with small thickness or phase modulation. Gao et al. [33] also proposed a different parallel two-step phase-shifting technique, in which two Ronchi gratings are used in tandem to form two parallel copies of the object and the reference beams. The successful operation of the technique would depend on the effectiveness of the phase grating. They followed it by using two cube beam splitters and one cube beam splitter setups where a quarter wave plate (QWP) and half wave plate (HWP) are placed in front of the detector for simultaneous recording of the phase-shifted holograms [34,35]. Since the spatial extent of the two beams that are derived from the cube splitter are generally very close, as they use a single CCD detector, precise size and positioning of the QWP and HWP is very critical. Furthermore, the above mentioned techniques record the two holograms using the same detector and hence place limitation on the size of the object to be investigated.

In this paper, we present a new parallel-quadrature phase-shifting DHM (PPS-DHM) based on a polarization beam splitter (PBS). A circularly polarized object beam is interfered with 45° polarized reference beam in the slightly off-axis geometry and the two quadrature phase-shifted holograms are recorded simultaneously at the transmitted and reflected beam paths of the PBS. We present reconstruction results of both amplitude and phase objects, and also the effects of the size of frequency plane aperture on the reconstructed object information. The advantage of this technique, compared to other techniques that are discussed above, is that the system configuration is simple and does not require any special optical elements. Furthermore, since we use two identical CCD sensors to record the two holograms, the size of the object to be investigated is only limited by the CCD detector area. Additionally, the two quadrature phase-shifted holograms are recorded simultaneously without any time lag, thus offering the possibility to reduce phase errors caused by mechanical vibrations and air turbulence that occurs in temporal phase-shifting holography. Moreover, another important advantage of the proposed parallel-quadrature phase-shifting holography is that it is built with simple polarization based optical components.

2. Experimental setup

An optical wave is in quadrature with another wave if they are matched in frequency and amplitude but differ in phase by 90°. The quadrature detection technique has been used to measure the amplitude and phase of an unknown signal by mixing with two reference signals that are in quadrature. We utilize this quadrature detection in digital holographic microscopy to measure the amplitude and quantitative phase information of microscopic objects. The schematic of the PPS-DHM with slightly off-axis geometry is shown in Fig. 1. Linearly polarized light from Ar–Kr laser ($\lambda=0.488\ \mu\text{m}$) is used in a Mach–Zehnder interferometer. This linearly polarized beam is initially converted into a circularly

polarized beam by using a QWP. The optical beam is then expanded and collimated. A non-polarizing beam splitter (NPBS₁) divides the beam into reference and object beam paths. The specimen is placed in the object beam path and the transmitted light is collected by a 20× microscope objective (MO) and collimated by lens L₂. A linear polarizer oriented at 45° relative to the \vec{x} and \vec{y} basis vectors is placed in the reference beam path to ensure that the reference beam is polarized at 45° before mixing with the object beam. In order to achieve slightly off-axis configuration, a very small angle between the object and reference beam is introduced by adjusting the mirror M₁ or beam splitter NPBS₂. The non-polarizing beam splitter (NPBS₂) is used to recombine the 45° linearly polarized reference beam with the circularly polarized object beam. The output from the NPBS₂ travels through a polarizing beam splitter (PBS) to separate into the quadrature components. The quadrature phase shift between the two interferograms is explained as follows: In the object beam arm the horizontal and the vertical components of the light has 90° phase difference between them. On the other hand, in the reference arm there is no phase difference between the horizontal and the vertical components. So, when the beams are combined by PBS, there is $\alpha=90^\circ$ shift between the interference pattern formed by the horizontal components and the interference pattern formed by the vertical components. Two identical CCD sensors (IDS UI1488LE-M, pixel size 2.2 μm , frame rate: 6 fp s) are used to record these quadrature phase-shifted holograms in parallel without any time lag. We used a LabVIEW VI to capture the two holograms from the two CCD sensors without any time lag. For the alignment purposes, the two CCDs are placed in x – y – z translation stages together with 360° rotation stages. The rotation axis is along the direction of propagation of the object beam. At first the distances between the PBS and the two CCDs are carefully adjusted to be equal. Direct images of an amplitude object are then grabbed by the two CCDs. The z micrometer translation stages are used to correct the defocusing error between the two images. Any lateral shift between the two images are also removed by using the combination of x and y micrometer stages. Finally, the alignment is checked by subtracting the images one from the other. This alignment procedure between the two CCD images is very essential for error-free reconstruction of the object information.

3. Reconstruction method

The two recorded quadrature phase-shifted holograms can be expressed as

$$I_1(x,y) = |O|^2 + |R|^2 + O^*R + OR^*, \quad (1)$$

$$I_2(x,y) = |O|^2 + |R|^2 + \exp(i\pi/2)O^*R + \exp(-i\pi/2)OR^* \quad (2)$$

where, $O(x,y)$ and $R(x,y)=A_r \exp(i2\pi qx)$ represent the object and reference beam complex amplitudes. q denotes the spatial carrier frequency introduced by the angle between the object and the reference waves. This spatial carrier frequency is kept the same for the both the holograms. The square terms are the dc components from the irradiance of the individual object and reference beams.

The dc terms $|O|^2 + |R|^2$ from the two holograms can be eliminated by subtracting Eq. (1) from Eq. (2) which gives rise to $I(x,y)$ as follows,

$$I(x,y) = I_2 - I_1 = [\exp(i\pi/2) - 1]O^*R + [\exp(-i\pi/2) - 1]OR^* \quad (3)$$

Next, the real image OR^* is separated from the twin image O^*R by standard technique of Fourier plane spatial filtering [11]. We perform a Fourier transform on $I(x,y)$. The frequency spectrum of

the real image is then centered in the Fourier plane which is similar to the effect of multiplying the dc-subtracted hologram by a digital reference wave R_D which is conjugate to the original reference wave. The information of the real image ($O(x,y)$) of the object can be obtained by selecting only the central region of this shifted Fourier spectrum. The term $[\exp(-i\pi/2)-1]$ associated with the real image only introduces a constant phase shift to the object wave and hence does not influence the phase distribution of the tested specimen. Finally, the complex amplitude of the object in the image plane is obtained by performing an angular spectrum based propagation operation on $O(x,y)$

$$O(x,y,d) = IFT \left\{ FT \{ O(x,y) \} \times \exp \left(i \frac{2\pi}{\lambda} d \sqrt{1 - (\lambda\xi)^2 - (\lambda\eta)^2} \right) \right\} \quad (4)$$

where, d is the distance between the image plane and the hologram plane. $FT\{\cdot\}$ and $IFT\{\cdot\}$ denote the Fourier transform and the inverse Fourier transform operator, respectively. ξ and η are spatial coordinates in the Fourier domain.

4. Experimental results

In this section, we present the experimental results performed with the experimental configuration shown in Fig. 1. The two parallel-quadrature phase-shifted holograms are recorded using the slightly off-axis geometry with the two detectors CCD1 and CCD2. The advantages of slightly off-axis recording geometry in comparison to traditional off-axis and in-line recording geometries are presented theoretically in Refs. [31–33]. It offers two distinct advantages compared to the traditional DHM techniques. Object reconstruction with slightly off-axis recording geometry can be performed with a detector of much lower spatial frequency bandwidth than that needed for traditional off-axis DHM. It also requires fewer measurements than traditional phase-shifting DHM. In slightly off-axis configuration the reference wave has a very small angle with respect to the object wave. Fig. 2(a) and (b) shows the two quadrature phase-shifted holograms for an amplitude object. Fig. 2(c) shows the resultant hologram after subtracting the two quadrature phase-shifted hologram from each other. Since the angle between the two beams is very small, the frequency spectrum of the dc term (which has twice the spectrum width of the real image or virtual image) overlaps with that of the real and twin images. This can be seen in Fig. 3(a) which shows the frequency spectrum of the hologram shown in Fig. 2(a). We have kept a small angle so that there is a strong overlap between the frequency spectra according to the concept of slightly off-axis holography. For the parallel-quadrature phase-shifting holography, the dc term is eliminated by subtracting the two phase-shifted holograms from each other (using Eq. (3)) and the corresponding

frequency spectrum is shown in Fig. 3(b). Comparing Fig. 3(a) and (b), we can see that the dc term can be removed by subtracting the two quadrature phase-shifted holograms recorded using two identical CCD sensors using the proposed configuration. The residual dc information and the two frequency maxima near the zero-order intensity in Fig. 3(b) can be attributed to the undesired parasitic interference patterns present in both Fig. 2(a) and (b). This can be ascribed to the parallel parasitic interferences due to the collimated illumination of the sample. Such artifacts may be reduced by using non-collimated illumination generated by a condenser lens. It should also be noted that, for the investigated objects, it would have been possible to choose a higher off-axis angle in the holograms to separate the different frequency spectra. However, in order to prove the efficacy of the proposed method, we have purposely kept a small off-axis angle so that there is strong overlap between the different frequency spectra.

Fig. 4 shows the reconstructed results for an amplitude object with a single off-axis hologram and Fig. 5 shows the reconstructed results using the two quadrature phase-shifted holograms. In Figs. 4(d) and 5(d), the frequency spectra corresponding to the real image are centered in the Fourier plane. This process is similar to the hologram being multiplied with a digital reference wave R_D (conjugate to the original reference wave) as required in the reconstruction of off-axis holograms. The spectrum of the real image is then selected by using a suitable spatial filter. One main factor that limits the quality of the reconstructed image in traditional off-axis DHM is the size and shape of the spatial filter [36]. The size and shape of the spatial filter has to be determined according to the distribution of spectrum of the object and its separation from the spectrum of the dc term. Fig. 4(a)–(c) shows the one-dimensional (1-D) plots (dotted red lines) of the reconstructed amplitude object for different sizes of the spatial filter using a single off-axis hologram. The reconstructed images are also shown in Fig. 4(a)–(c). The different spatial filters used are shown in Fig. 4(d) and the 1-D plots are shown in the order of increasing size of the filter. The dotted blue lines in Fig. 4(a)–(c) show the 1-D plot of the direct image of the amplitude object for comparison with the reconstructed object. It is clear that the reconstructed object quality depend strongly on the size of the spatial filter. Fig. 5(a)–(c) shows the 1-D plot (dotted red lines) of the reconstructed object using the two parallel-quadrature phase-shifted holograms. The different spatial filters used are shown in Fig. 5(d). The dotted blue lines in Fig. 5(a)–(c) show the 1-D plot of the direct image of the amplitude object. Here we notice that with increase in size of the frequency plane spatial filter, the matching between the direct image and the reconstructed object information improves. This shows the improved reconstruction capability of the parallel-quadrature phase-shifting DHM. Furthermore, in the case of PPS-DHM, the maximum allowable size of the spatial

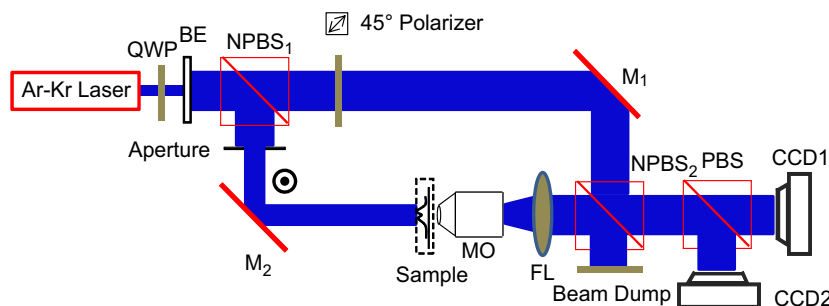


Fig. 1. Experimental configuration to perform digital holographic microscopy using parallel-quadrature phase-shifting method. QWP, quarter wave plate; BE, beam expander; NPBS, non-polarizing beam splitter; MO, microscope objective; M, mirror; PBS, polarizing beam splitter; CCD, charge coupled device detectors; FL, field lens. CCD1 and CCD2 are controlled using LabVIEW.

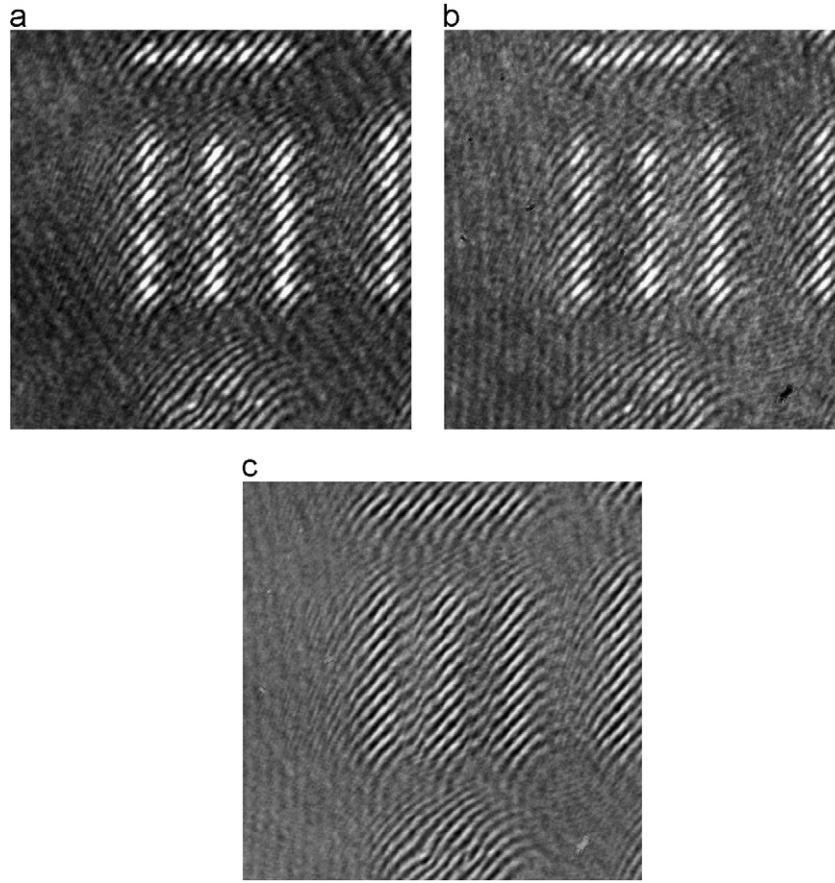


Fig. 2. (a) and (b) Two quadrature phase-shifted holograms recorded by using CCD1 and CCD2. (c) The subtracted hologram.

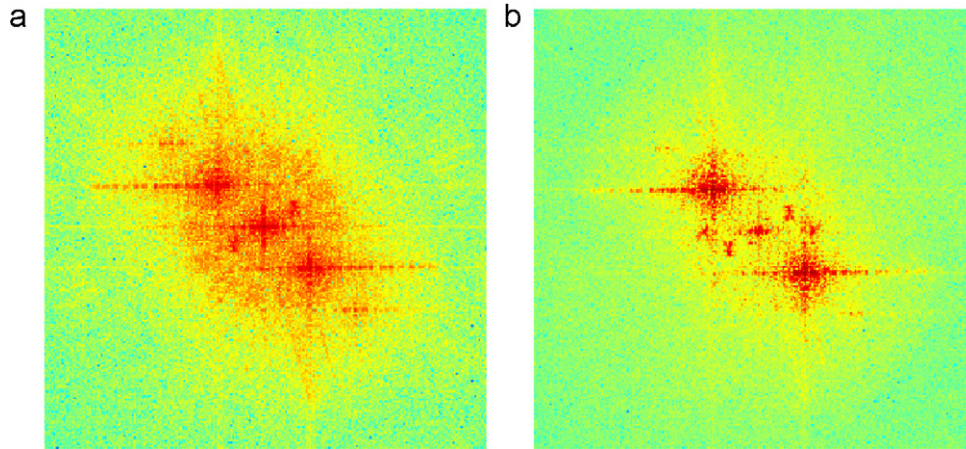


Fig. 3. (a) Spatial frequency spectrum of the hologram shown in Fig. 2(a) and (b) spatial frequency spectrum after subtracting the two quadrature phase-shifted holograms.

filter is determined by the separation between the frequency spectra of real and twin images. Without the loss of generality, this spatial filter can be represented by a circle with a diameter equal to the separation between the frequency spectra of the real and twin image, and centered on the frequency spectra of the real image. If μ is the separation between the frequency spectra of real and twin images, then the aforementioned spatial filter can be represented by,

$$H(\xi, \eta) = \frac{(\xi - \xi_0)^2 + (\eta - \eta_0)^2}{(\mu/2)^2} \quad (5)$$

where, (ξ_0, η_0) is the center of the frequency spectra of the real image. ξ, η are the spatial coordinates in the Fourier domain.

In Figs. 4(d) and 5(d), the largest spatial filter shows this circle. Thus, PPS-DHM with slightly off-axis configuration allows us to choose a spatial filter with much larger dimension than traditional off-axis DHM which leads to better reconstruction capability as shown in the experimental results. Next we demonstrate the phase object reconstruction with the proposed method. Fig. 6 shows the reconstructed quantitative phase of a glass bead (Polysciences, 10–30 μm) in Citra mounting media. Glass beads are uniformly mixed in Citra mounting media and placed between a microscopic

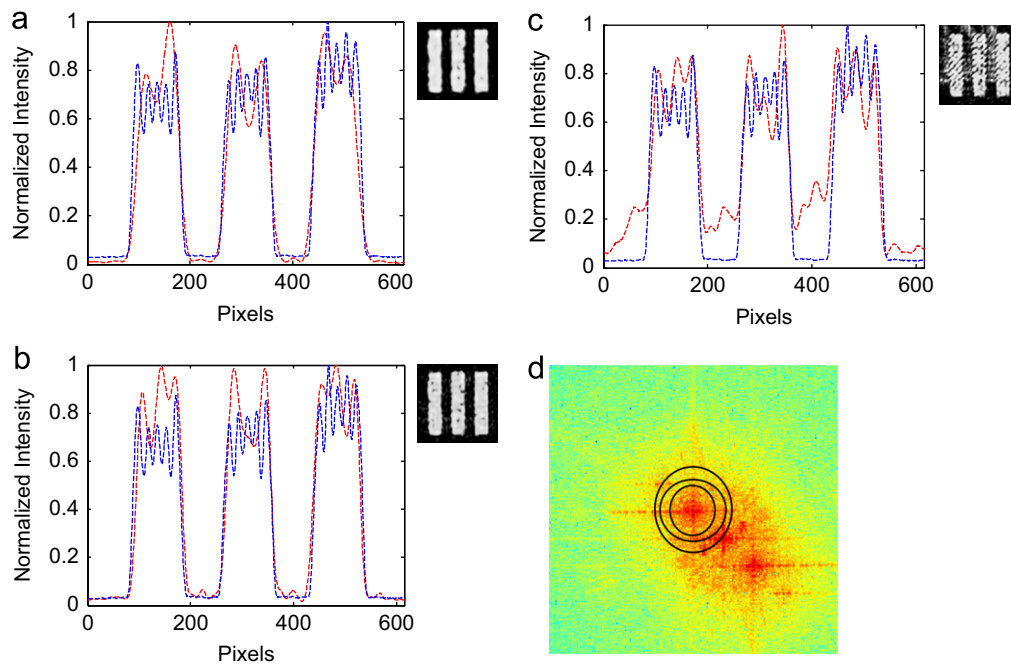


Fig. 4. Reconstructed amplitude object information using a single off-axis hologram. Dotted red lines show 1-D plots of the reconstructed amplitude object for different sizes of the spatial filter. The dotted blue lines show the 1-D plot of the direct image of the amplitude object. (a)–(c) is in order of increasing size of the spatial filter shown in (d). The reconstructed object quality depends strongly on the size of the spatial filter. (For interpretation of the references to color in this figure caption, the reader is referred to the web version of this article.)

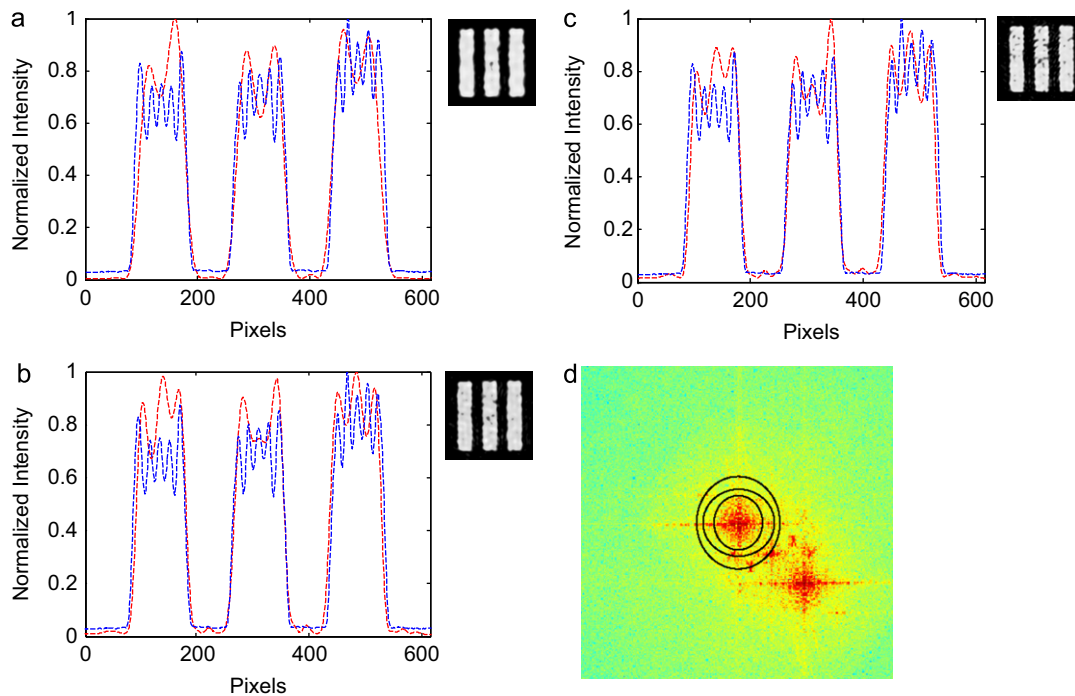


Fig. 5. Reconstructed amplitude object information using the two quadrature phase-shifted holograms. Dotted red lines show 1-D plots of the reconstructed amplitude object for different sizes of the spatial filter. The dotted blue lines show the 1-D plot of the direct image of the amplitude object. (a)–(c) is in order of increasing size of the spatial filter shown in (d). The matching between the direct image and the reconstructed object information improves with increase in size of the spatial filter. (For interpretation of the references to color in this figure caption, the reader is referred to the web version of this article.)

slide and a cover slip. The refractive index of the glass beads is 1.51 and that of Citra mounting media is 1.484 at 20 °C. Fig. 6(a) shows the reconstruction result with a single off-axis hologram and Fig. 6(b) is the reconstruction result with PPS-DHM technique. The vertical color bar shows the phase values in radians.

Fig. 6(c) shows the comparison of the reconstructed phase profile of the glass bead. We notice a smoother reconstruction phase profile for the PPS-DHM technique. Moreover, the background phase fluctuation is smaller in the case of PPS-DHM. Fig. 6(d) shows the background phase values in radians along the yellow lines in

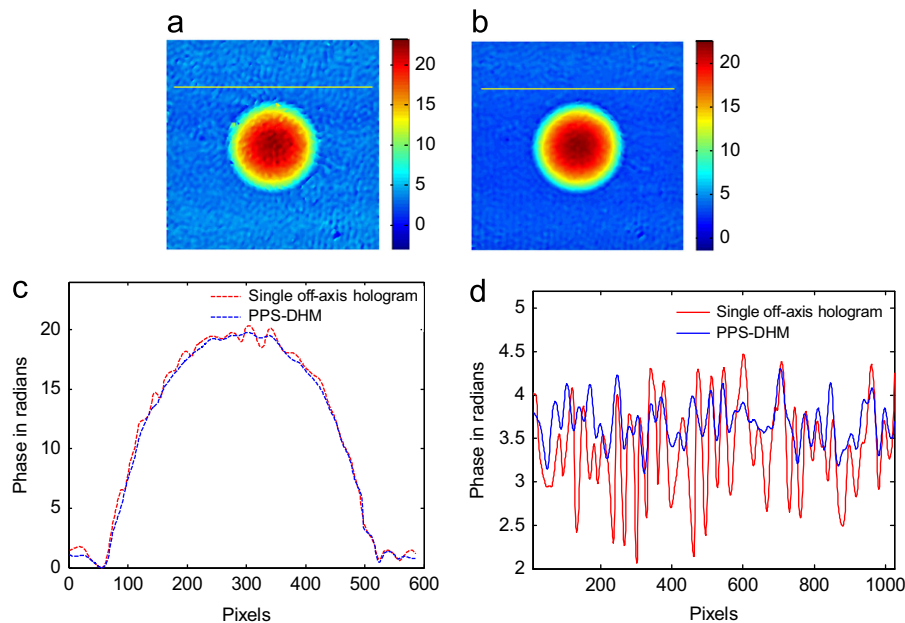


Fig. 6. Reconstructed quantitative phase image of a glass bead. (a) Single off-axis hologram and (b) PPS-DHM. The vertical color shows the phase values in radians. (c) Comparison of the reconstructed phase profile of the glass beads shown in (a) and (b). A smoother reconstruction phase profile is recovered for the PPS-DHM technique. (d) Background phase values along the yellow lines shown in (a) and (b). The standard deviation of this background phase fluctuation is 0.52 rad for single off-axis hologram and 0.24 rad for PPS-DHM technique. (For interpretation of the references to color in this figure caption, the reader is referred to the web version of this article.)

Fig. 6(a) and (b). The standard deviation of this background phase fluctuation is 0.52 rad for single off-axis hologram and 0.24 rad for PPS-DHM technique. This shows that the dc term can be very efficiently removed by subtracting the two quadrature phase-shifted holograms and demonstrates the applicability of the proposed PPS-DHM technique. The background noise can be further reduced by statistical averaging technique since the coherent disturbances in the two recorded holograms are slightly different.

5. Conclusions

In conclusion, we present a new configuration to perform parallel two-step phase-shifting holography for DHM using the principle of polarization phase-shifting. Two quadrature phase-shifted holograms are simultaneously recorded by two identical CCD sensors at the reflected and transmitted beam paths of a polarizing beam splitter using the slightly off-axis recording geometry. The dc term is successfully suppressed by subtracting one phase-shifted hologram from the other, and the object information is reconstructed by selecting the frequency spectrum of the real image. The simultaneous recording of two holograms offers the possibility to eliminate phase errors resulting from mechanical vibrations and air turbulence occurring in temporal phase-shifting holography. Experimental results of amplitude and phase objects demonstrate that a much larger dimension of the spatial filter can be used in this design which is determined by the separation between the frequency spectra of the real and virtual image. This leads to better reconstruction capability than traditional off-axis holographic microscopy. In addition the technique of parallel phase-shifting slightly off-axis DHM results in lower noise than the traditional off-axis DHM because common phase noise is eliminated in the intensity subtraction of the two parallel-quadrature phase-shifted holograms. Furthermore, the proposed configuration requires lower detector bandwidth than traditional off-axis DHM and fewer measurements than traditional phase-shifting in-line DHM.

Acknowledgments

This work is supported by National Center for Research Resources, NIH, Grant No. 1R21RR024429-01A1.

References

- [1] E. Cuche, P. Marquet, C. Depeursinge, *Applied Optics* 38 (1999) 6994.
- [2] P. Marquet, B. Rappaz, P.J. Magistretti, E. Cuche, Y. Emery, T. Colomb, C. Depeursinge, *Optics Letters* 30 (2005) 468.
- [3] M.K. Kim, "Principles and techniques of digital holographic microscopy," *SPIE Reviews* 1, 018005-1/50 (2010).
- [4] F. Charrière, A. Marian, F. Montfort, J. Kühn, T. Colomb, E. Cuche, P. Marquet, C. Depeursinge, *Optics Letters* 31 (2006) 178.
- [5] B. Das, C.S. Yelleswarapu, *Optics Letters* 35 (2010) 3426.
- [6] B. Rappaz, A. Barbul, A. Hoffmann, D. Boss, R. Korenstein, C. Depeursinge, P.J. Magistretti, P. Marquet, *Blood Cells, Molecules, and Diseases* 42 (2009) 228.
- [7] L. Yu, S. Mohanty, J. Zhang, S. Genc, M.K. Kim, M.W. Berns, Z. Chen, *Optics Express* 17 (2009) 12031.
- [8] M. Antkowiak, M.L. Torres-Mapa, K. Dholakia, F.J. Gunn-Moore, *Optics Express* 1 (2010) 414.
- [9] T. Colomb, N. Pavillon, J. Kuhn, E. Cuche, C. Depeursinge, Y. Emery, *Optics Letters* 35 (2010) 1840.
- [10] U. Schnars, W. Juptner, *Applied Optics* 33 (1994) 179.
- [11] E. Cuche, P. Marquet, C. Depeursinge, *Applied Optics* 39 (2000) 4070.
- [12] L. Xu, X. Peng, Z. Guo, J. Miao, A. Asundi, *Optics Express* 13 (2005) 2444.
- [13] L. Xu, J. Miao, A. Asundi, *Optical Engineering* 39 (2000) 3214.
- [14] N.T. Shaked, T.M. Newpher, M.D. Ehlers, A. Wax, *Applied Optics* 49 (2010) 2872.
- [15] D. Carl, B. Kemper, G. Wernicke, G. von Bally, *Applied Optics* 43 (2004) 6536.
- [16] J. Yamaguchi, S. Kato, Ohta, J. Mizuno, *Applied Optics* 40 (2001) 6177.
- [17] C.P. Brophy, *Journal of the Optical Society of America A* 7 (1990) 537.
- [18] J. Schwider, R. Burrow, K.-E. Elssner, J. Grzanna, R. Spolaczyk, K. Merkel, *Applied Optics* 22 (1983) 3421.
- [19] C.S. Gao, L. Zhang, H.T. Wang, J. Liao, Y.Y. Zhu, *Optics Letters* 31 (2002) 1687.
- [20] J. Schmit, K. Creath, *Applied Optics* 34 (1995) 3610.
- [21] R. Smythe, R. Moore, *Optical Engineering* 23 (1984) 361.
- [22] C.L. Koliopoulos, *Proceedings of SPIE* 1531 (1992) 119.
- [23] N.R. Sivakumar, W.K. Hui, K. Venkatakrishnan, B.K.A. Ngoi, *Optical Engineering* 42 (2003) 367.
- [24] D.J. Townsend, K.D. Quarles, A.L. Thomas, W.S. Rockward, C.M. Warner, J.A. Newmark, C.A. DiMarzio, *Proceedings of SPIE* 4964 (2003) 59.
- [25] W.S. Rockward, A.L. Thomas, B. Zhao, C.A. DiMarzio, *Applied Optics* 47 (2008) 1684.
- [26] M. Novak, J. Millerd, N. Brock, M. North-Morris, J. Hayes, J. Wyant, *Applied Optics* 44 (2005) 6861.

- [27] Y. Awatsuji, T. Tahara, A. Kaneko, T. Koyama, K. Nishio, S. Ura, T. Kubota, O. Matoba, *Applied Optics* 47 (2008) D183.
- [28] T. Kakue, Y. Moritani, K. Ito, Y. Shimozaoto, Y. Awatsuji, K. Nishio, S. Ura, T. Kubota, O. Matoba, *Optics Express* 18 (2010) 9555.
- [29] N.-I. Toto-Arellano, G. Rodriguez-Zurita, C. Meneses-Fabian, J. Vazquez-Castillo, *Optics Express* 16 (2008) 19330.
- [30] C. Meneses-Fabian, G. Rodriguez-Zurita, M. Encarnacion-Gutierrez, N.-I. Toto-Arellano, *Optics Communications* 282 (2009) 3063.
- [31] N.T. Shaked, Y. Zhu, M.T. Rinehart, A. Wax, *Optics Express* 17 (2009) 15585.
- [32] N.T. Shaked, M.T. Rinehart, A. Wax, *Optics Letters* 34 (2009) 767.
- [33] P. Gao, B. Yao, I. Harder, J. Min, R. Guo, J. Zheng, T. Ye, *Journal of the Optical Society of America A* 28 (2011) 434.
- [34] P. Gao, B. Yao, J. Min, R. Guo, J. Zheng, T. Ye, I. Harder, V. Nercissian, K. Mantel, *Optics Express* 19 (2011) 1930.
- [35] P. Gao, B. Yao, J. Min, R. Guo, J. Zheng, T. Ye, *Optics Communications* 284 (2011) 4136.
- [36] J. Weng, J. Zhong, C. Hu, *Applied Optics* 49 (2010) 189.